Journal of Molecular Structure 1051 (2013) 205–210

Contents lists available at ScienceDirect

Journal of Molecular Structure

journal homepage: www.elsevier.com/locate/molstruc

Catena-(bis((1,10-phenanthroline-N,N′)-copper(II)) hydroxy-bis (phosphato)-tris(dioxo-vanadium(v))): A polymorphic phase driven by disorder

Cristian Silva-Galaz [a,b], Marianela Saldías [b,c], Eleonora Freire [d,e,*], Ricardo Baggio [d], E. Le Fur [f,g], Verónica Paredes-Garcia [b,h], Evgenia Spodine [b,i], Diego Venegas-Yazigi [a,b,*]

[a] Facultad de Química y Biología, Universidad de Santiago de Chile, USACH, Santiago, Chile
[b] CEDENNA, Santiago, Chile
[c] Facultad de Ciencias Físicas y Matemáticas, Universidad de Chile, Santiago, Chile
[d] Gerencia de Investigación y Aplicaciones, Centro Atómico Constituyentes, Comisión Nacional de Energía Atómica, Buenos Aires, Argentina
[e] Escuela de Ciencia y Tecnología, Universidad Nacional General San Martín, Buenos Aires, Argentina
[f] ENSCR, CNRS, UMR 6226, Rennes, France
[g] Université Européenne de Bretagne, UMR 6226, France
[h] Facultad de Ciencias Químicas y Farmacéuticas, Universidad de Chile, Santiago, Chile
[i] Universidad Andres Bello, Departamento de Ciencias Químicas, Santiago, Chile

HIGHLIGHTS

- A crystallographic study of $[Cu_6(phen)_6(V^VO_2)_6(PO_4)_6(V^VO_2HO)_3]$.
- The crystal structure analysis suggests that this can be one of a large number of polymorphic states with structural differences.
- The pseudo symmetry problem defining the polymorphic states is discussed.
- A magnetic characterization of (**1a**) was performed, showing that the compound is antiferromagnetic.

ARTICLE INFO

Article history:
Received 15 May 2013
Received in revised form 5 August 2013
Accepted 5 August 2013
Available online 16 August 2013

Keywords:
Copper(II) phosphovanadate
Pseudosymmetry
Polymorphism
Magnetism

ABSTRACT

In the present paper a copper(II) phosphovanadate is presented and formulated as $[Cu_6(phen)_6(V^VO_2)_6(PO_4)_6(V^VO_2HO)_3]$ (**1a**). This compound was obtained by hydrothermal synthesis and crystallizes in the triclinic group P-1, with $a = 10.6290(5)$, $b = 17.4275(8)$, $c = 23.6151(11)$ Å; $\alpha = 92.888(4)°$, $\beta = 98.910(4)°$ and $\gamma = 91.995(4)°$. The *leitmotif* in (**1a**) is almost identical to some previously reported ones, viz. $[Cu(phen)(V^VO_2)(PO_4)]_2[V^VO_2(OH)]$ (**2**); $[Cu(phen)(V^VO_2)(PO_4)]_2[V^{IV}O_2(H_2O)]$ (**3**) except for the fact that the small cells found in (**2**)–(**3**) are tripled in (**1a**). The reasons driving to these differences are subtle, and reside in the way in which the disorder in some vanadate groups takes place, viz., completely at random in (**2**)–(**3**) thus leading to a small "average" cell, while keeping some systematics in (**1a**) thus needing for a larger *motif* to take account of its repetition scheme in the crystal. The magnetic unit in the structure of (**1a**) is defined by a dinuclear system of Cu^{II} bonded by a μ_2,η^1-PO_4 bridge. A fit of the corresponding magnetic data of (**1a**) was done, using the van Vleck equation for two $S = ½$ centres ($H = -J\hat{S}_a \cdot \hat{S}_b$). The parameters obtained by the fit of the experimental data were $g = 2.1$ and $J = -3.5$ cm^{-1}.

1. Introduction

Phosphovanadates (VPO) constitute a well explored type of compounds, which in spite of their long term studies persist in driving the attention of structural chemists due to their unpredictable structural diversity. This is the result of the variety of geometric surroundings, which the vanadium cation can adopt in its different oxidation states, as well as the way in which it can condense with the phosphate anion [1]. Besides the fact that functionalization of these oxides with transition metal complexes allows the generation of quite different structures and dimensionalities, like chains, lamellar or heavily interconnected three-dimensional arrays [2–10]. A final, non-minor ingredient in this structural "Pandora's box" is the finding that slight differences in synthetic conditions might derive in

* Corresponding authors. Addresses: Gerencia de Investigación y Aplicaciones, Centro Atómico Constituyentes, Comisión Nacional de Energía Atómica, Buenos Aires, Argentina. Tel.: +54 11 40824774 (E. Freire), Facultad de Quimica y Biologia. Universidad de Santiago de Chile, USACH, Casilla 40, correo 33, Santiago, Chile. Tel.:+562 27181079 (D. Venegas-Yazigi).
E-mail addresses: freire@tandar.cnea.gov.ar (E. Freire), diego.venegas@usach.cl (D. Venegas-Yazigi).

0022-2860/$ - see front matter © 2013 Elsevier B.V. All rights reserved.
http://dx.doi.org/10.1016/j.molstruc.2013.08.005

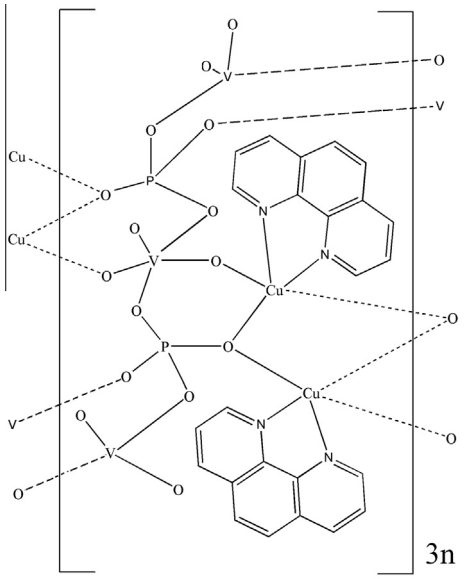

Scheme 1. Basic unit of (1a).

either subtle or important structural differences in the final products.

In this work an interesting example of the former case is presented. A detailed structural analysis of an organo-inorganic hybrid compound is discussed, corresponding to an inorganic VPO framework functionalized with a Cu^{II} complex having 1,10-phenanthroline (phen) as ligand, $[Cu_6(phen)_6(VO_2)_6(PO_4)_6(VO_2HO)_3]$ (**1a**) (Scheme 1) that was obtained by the hydrothermal method. Almost exact replicas of this structure had already been reported by Finn and Zubieta [4] and Zhang et al. [5], but as we shall discuss below, with some subtle differences setting them apart as different polymorphic structures.

The magnetic characterization shows that compound (**1a**) presents an antiferromagnetic behaviour due to the super-exchange interaction existing between Cu2 and Cu3 (3.262(3) Å).

2. Materials and methods

2.1. Synthesis

A mixture of $NaVO_3$ (0.156 g, 1.2 mmol), H_3PO_4 (0.098 g, 1.0 mmol), $Cu(NO_3)_2{\cdot}3H_2O$ (0.290 g, 1.20 mmol), 1,10-phenanthroline (0.198 g, 1.0 mmol) and H_2O (2.00 mL, 111 mmol) in a molar ratio of 1.2:1.0:1.2:1.0:111, was stirred for 1 h before being heated at 200 °C in a 23 mL Teflon Lined Parr reactor for 120 h. After cooling to room temperature, green crystals of $[Cu_6(phen)_6(VO_2)_6(PO_4)_6(VO_2HO)_3]$ (**1a**) where mechanically separated, washed and dried. The obtained yield in vanadium is 45%. The initial pH of the mixture was 1.8, and the final pH of the reaction mixture was 2.3.

2.2. SEM–EDXS

The presence of vanadium, phosphorous and copper atoms was determined by SEM–EDXS analysis using a SEM–EDX JSM 5410 equipment. Fig. 1S (Supplementary material) shows the micrography of some crystals and the EDX spectrum. The presence of Pd, and Au in the spectrum is due to the grid used in the experiment.

2.3. FTIR

Infrared spectrum of the powder sample was recorded in the 4000–400 cm^{-1} range at room temperature on a Perkin Elmer FTIR spectrophotometer, model BX II, using KBr pellets. The principal bands are (cm^{-1}): 898 (s), 987 (s) corresponding to terminal V=O and O—V—O bridge stretching modes; 1114 (s), 1164 (s) assigned to P=O and P—O groups; 1392 (m) and 1443 (m) assigned to C=C and C=N groups of the organic ligand (phen).

2.4. X-ray diffraction

Single crystal data were collected on an Oxford Diffraction Gemini diffractometer, Mo Kα radiation, and the following software was used in different stages of the crystal structure analysis process: Data collection: CrysAlis PRO (Oxford Diffraction, 2009) [11]; cell refinement: CrysAlis PRO; data reduction: CrysAlis PRO; program(s) used to solve structure: SHELXS97 [12]; program(s) used to refine structure: SHELXL97 [12]; molecular graphics: SHELXTL [12]; software used to prepare material for publication: SHELXL97, PLATON [13]. All H atoms were identified in a difference Fourier map, and further idealized and allowed to ride (C—H: 0.93 Å, O—H: 0.85 Å, U(H)isot = 1.2 × U(host).

The structure presents an important pseudo translation symmetry, broken by a differentiated splitting in a few, otherwise equivalent, vanadyl V—O's. The latter groups were refined with similar restraints (SADI and DELU in SHELXL), and their

Table 1
Comparison between (**1a**), (**1b**), (**2**).

Structure	(**1a**)	(**1b**)	(**2**)
# of Independent motives $[C_{24}H_{17}Cu_2N_4O_{15}P_2V_3]$	3	1/2	1/2
Mr	2829.77	471.63	471.63
S.G.	P-1	P-1	P-1
a (Å)	10.6290 (5)	10.6290 (5)	10.6203 (7)[a]
b (Å)	17.4275 (8)	17.4275 (8)	17.2324 (9)[a]
c (Å)	23.6151 (11)	8.0764 (4)	8.0547 (7)[a]
α (°)	92.888 (4)	135.229 (3)	135.140 (3)[a]
β (°)	98.910 (4)	57.374 (4)	56.959 (5)[a]
γ (°)	91.995 (4)	91.995 (4)	92.454 (13)[a]
V ($Å^3$)	4312.1 (4)	718.66 (6)	709.30 (10)
T (K)	291 (2)	291 (2)	90 (4)
Data: total, indep., $F^2 > 2\sigma(F^2)$	66556/20174/11094	11139/6295/5906	na/4786/na
h,*k*,*l* range	−14–14; −22–22; −31–32	−13–14; −22–22; −10–10	na
Parameters	1365	245	245
R_{equiv}	0.0239	0.0140	na
$\langle F^2/\sigma(F^2)\rangle$	39.2	71.4	na
$R[F^2 > 2\sigma(F^2)]$; $wR(F^2)$	0.0412; 0.1098	0.0238; 0.0670	0.0537; 0.1321
Occupation of central V atoms	0.8432/0.1568 (14) 1.00/0.00 0.8525/1475 (14)	0.50/0.50	0.50/0.50
$\Delta\rangle_{max}$; $\Delta\rangle_{min}$ ($eÅ^{-3}$)	0.38; −0.73	0.92; −0.75	na; na

na: not-available info.
[a] Cell axes transformed to facilitate comparison with those in (**1b**).

Table 2
Selected bond lengths for (**1a**) (Å).

Cu1—O32	1.957 (3)	V2′—O21	2.194 (4)
Cu1—O52	1.972 (3)	V2′—P2	2.905 (3)
Cu1—N2A	1.984 (3)	V2′—H72	1.8740
Cu1—N1A	2.015 (3)	O72—H72	0.8500
Cu1—O32^{i}	2.293 (3)	V3—O53	1.607 (3)
Cu2—O72	1.929 (2)	V3—O63	1.608 (3)
Cu2—O31	1.963 (3)	V3—O41^{iv}	1.860 (3)
Cu2—N2B	2.010 (3)	V3—O12	1.866 (3)
Cu2—N1B	2.012 (3)	V4—O54	1.603 (3)
Cu2—O34	2.331 (3)	V4—O64	1.612 (3)
Cu3—O65	1.963 (2)	V4—O44^{iii}	1.863 (3)
Cu3—O34	1.965 (3)	V4—O13	1.865 (2)
Cu3—N2C	1.988 (3)	V5—O55	1.599 (3)
Cu3—N1C	2.012 (3)	V5—O65	1.711 (3)
Cu3—O31	2.259 (3)	V5—O23	1.956 (2)
Cu4—O75	1.935 (2)	V5—O75	1.964 (3)
Cu4—O33	1.972 (3)	V5—O24	1.980 (3)
Cu4—N2D	2.019 (3)	O75—H75	0.8500
Cu4—N1D	2.019 (3)	V6—O56	1.610 (3)
Cu4—O36	2.328 (3)	V6—O66	1.610 (3)
Cu5—O58	1.963 (2)	V6—O43^{iv}	1.862 (3)
Cu5—O36	1.967 (3)	V6—O14	1.864 (3)
Cu5—N2E	1.985 (3)	V7—O57	1.609 (3)
Cu5—N1E	2.005 (3)	V7—O67	1.611 (3)
Cu5—O33	2.256 (3)	V7—O46^{iii}	1.856 (3)
Cu6—O78	1.935 (3)	V7—O15	1.858 (3)
Cu6—O35	1.972 (3)	V8—O68	1.599 (3)
Cu6—N2F	2.013 (3)	V8—O58	1.695 (3)
Cu6—N1F	2.015 (3)	V8—O25	1.928 (2)
Cu6—O35^{ii}	2.302 (3)	V8—O78	1.939 (3)
V1—O61	1.606 (3)	V8—O26	2.025 (3)
V1—O51	1.611 (3)	V8′—O68′	1.589 (9)
V1—O42^{iii}	1.857 (3)	V8′—O78	1.605 (4)
V1—O11	1.863 (3)	V8′—O26	1.834 (4)
V2—O62	1.596 (3)	V8′—O58	1.893 (4)
V2—O52	1.675 (3)	V8′—O25	2.158 (4)
V2—O21	1.910 (2)	V8′—H78	2.0829
V2—O72	1.983 (3)	O78—H78	0.8500
V2—O22	2.044 (3)	V9—O59	1.612 (3)
V2′—O72	1.575 (4)	V9—O69	1.613 (3)
V2′—O62′	1.589 (9)	V9—O45^{iv}	1.858 (3)
V2′—O22	1.776 (4)	V9—O16	1.859 (3)
V2′—O52	1.950 (4)		

Symmetry codes: (i) $-x+2,-y,-z$; (ii) $-x,-y+2,-z+1$; (iii) $x-1,y,z$; and (iv) $x+1,y,z$.

Table 3
Hydrogen-bond geometry for (**1a**) (Å, °).

D—H···A	D—H	H···A	D···A	D—H···A
C3A—H3A···O68^{v}	0.93	2.59	3.356 (5)	140
C5A—H5A···O68^{v}	0.93	2.31	3.152 (6)	151
C5C—H5C···O55^{v}	0.93	2.36	3.216 (5)	153
C5E—H5E···O62^{v}	0.93	2.31	3.162 (5)	153
C8A—H8A···O69^{v}	0.93	2.45	3.318 (6)	156
C8B—H8B···O67^{vi}	0.93	2.39	3.276 (6)	158
C8C—H8C···O66^{v}	0.93	2.48	3.350 (5)	155
C8D—H8D···O64^{vi}	0.93	2.39	3.270 (5)	158
C8E—H8E···O63^{v}	0.93	2.47	3.344 (5)	156
C8F—H8F···O61^{vi}	0.93	2.42	3.309 (6)	159
C6B—H6B···O15^{vi}	0.93	2.58	3.472 (5)	162
C6D—H6D···O13^{vi}	0.93	2.57	3.463 (5)	161
C6F—H6F···O11^{vi}	0.93	2.60	3.493 (5)	161

Symmetry codes: (v) $-x+1,-y+1,-z$ and (vi) $-x+1,-y+1,-z+1$.

occupation factors converged to V2—O62: 0.8432/0.1568 (14), V8—O68:0.8525/0.1475 (16).

Table 1 (first column) presents the crystal data and structure refinement parameters for (**1a**). Further information on structural details on the structure can be found in Table 2 (coordination distances) and Table 3 (H-bonding interactions).

2.5. Magnetic measurements

The magnetization was measured over the temperature range of 2–300 K for (**1a**). Measurements were performed on 73.7 mg at 1 kOe, using a Quantum Design SQUID magnetometer (MPMS-XL5). Diamagnetic corrections of the constituent atoms were estimated from Pascal constants [14]. The validity of the fitting procedure for the used model in this work was done using the agreement factor, defined as:

$$R = \sum [(\chi_M T)_{exp} - (\chi_M T)_{calc}]^2 \Big/ \sum [(\chi_M T)_{exp}]^2$$

The molar magnetic data of (**1a**) were obtained using the formula weight determined by crystallography, that is, with six spin carriers per mole.

3. Results and discussion

Fig. 1 presents an ellipsoid plot of the compound. The complexity of the structure (apparent from inspection) is the result of a frustrated threefold translation symmetry along the $\langle 1/3,-1/3,-1/6\rangle$ vector which makes the asymmetric unit three times as

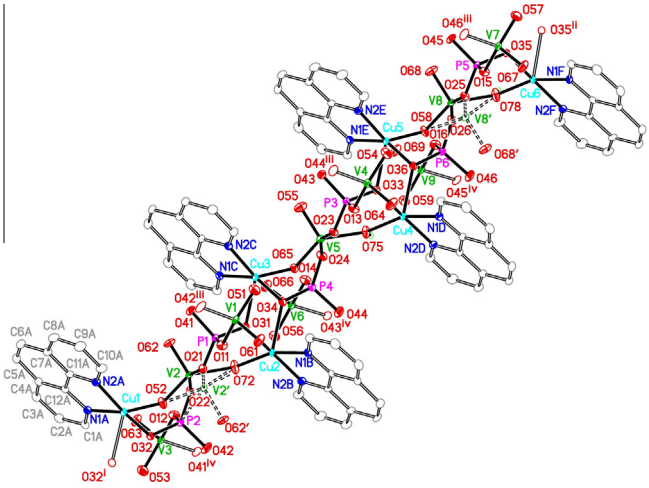

Fig. 1. Molecular view of (**1a**) with displacement ellipsoids at a 30% level. Carbon atoms in the phen groups "B" to "F" are not labelled in the figure, but repeat the labelling scheme as those in the "A" moiety. Aromatic H atoms omitted. Symmetry codes: (i) $-x+2,-y,-z$; (ii) $-x,-y+2,-z+1$; (iii) $x-1,y,z$; and (iv) $x+1,y,z$.

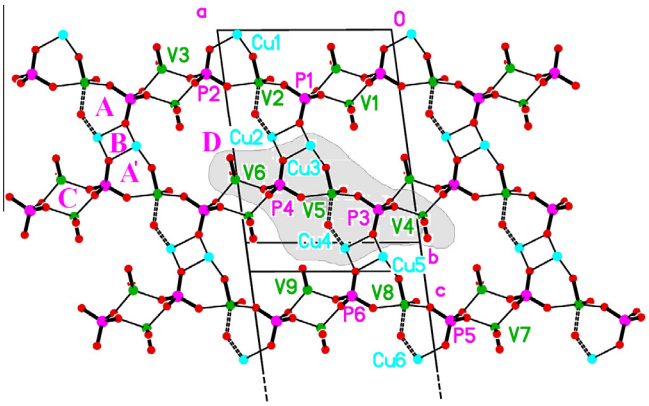

Fig. 2. The inorganic 2D structure in a view normal to (011) (phenligands and H atoms removed, for clarity). Line codes: full heavy lines: $O_{vanadyl}$, $O_{phosphate}$ covalent bonds; full weak lines: $O_{vanadyl}$, $O_{phosphate}$ coordination bonds; strong broken lines: $O_{Hydroxyl}$ coordination bonds.

large as it would be required if the proper symmetry were in force. This means that, in a first order approximation the structure of (**1a**) can be considered as a triple *leitmotif* with very minor variations from one another, or in other words and from a purely crystallographic point of view, (**1a**) is approximately $\{[Cu_2(phen)_2(PO_4)_2][(VO_2)_2(VO_2HO)]\}_3$. (See below for a thorough discussion on this pseudo symmetry.) The pseudo "elemental" unit is highlighted in Fig. 2, where a schematic view of the resulting 2D structure is presented with the phenligands removed, for clarity.

As can be observed from both Figs. 1 and 2, each "elemental" unit is formed by two copper Cu^{II} and three vanadyl $\left(V^{V}O_2^{+}\right)$ groups, charge balanced by two phosphate $\left(PO_4^{3-}\right)$ and one hydroxyl (OH^-) groups. The relevant atoms characterizing each group in the three moieties are in an ordered sequence: {Cu1, Cu2; V1, V2, V3; P1, P2; O72}; {Cu3, Cu4; V4, V5, V6; P3, P4; O75} and {Cu5, Cu6; V6, V7, V8; P5, P6; O78} with Cu1 being the "quasi equivalent" to Cu3 and Cu5, and so on.

Both copper cations in each unit have a similar square pyramidal geometry, and both are chelated by the phen ligands, through the corresponding N atoms (N1, N2) A, B, to (N1, N2) E, F with Cu—N distances of 1.984 (3)–2.019 (3) (Table 2). The oxygen atoms that bind the copper centres correspond to two phosphate and one vanadyl group (Cu1, Cu3 and Cu5). The apical bond corresponds to one of the vanadyl oxygen atoms (Cu—O_{apical}: 2.226 (3)–2.351 (3) Å) with basal Cu—O_{phosp}, Cu—$O_{vanadyl}$ being shorter and very similar, spanning the tight range 1.957 (3)–1.972 (3) Å. A hydroxyl group replaces the vanadyl oxygen in Cu2, Cu4 and Cu6.

There are two different coordination types within the vanadium cations in each group: the outermost ones V1, V3; V4, V6; V7, V9 are similar to each other with a fourfold, deformed tetrahedral coordination, fulfilled by its two intrinsic vanadyl plus two phosphate oxygen atoms. Both groups of bonds are similar in the three "pseudo equivalent" units, but different from each other (V—$O_{vanadyl}$: 1.603 (3)–1.613 (3) Å, V—$O_{phosphate}$: 1.856 (3)–1.866 (3) Å). The central vanadium cations, V2, V5 and V8, present instead a fivefold coordination by inclusion of a hydroxyl group, which completes a deformed square pyramidal arrangement where vanadyl bonds are also shorter than the phosphate/hydroxyl ones. In all cases, their internal spread is larger than in the previous group (V—$O_{vanadyl}$ range: 1.596(3)–1.711(3) Å, V—O_{rest}: 1.910(3)–2.044(3) Å). It is important to note for future reference, that the V2—O62, V8—O68 groups appear as slightly disordered, through splitting at both sides of the basal plane of the corresponding pyramid, with a local change of chirality.

Occupation factors were independently refined for both groups, and converged to very similar final values (V2—O62: 0.8432 (14/0.1568 (14), V8—O68:0.8525 (14), 0.1475 (14)). On the other hand, the V5—O65 group did not show any appreciable splitting. The PO_4^{3-} groups are featureless, with an even span of P—O distances (1.514 (3)–1.555 (3) Å) for the six independent moieties.

The planar inorganic 2D structure evolves parallel to (0 −1 1) (Fig. 2). The network presents five different kind of loops of general type $(M—O)_n$, where M stands for either Cu, V or P, two of them with $n = 3$ (A, A′ in Fig. 2) and three with $n = 2$, 4 and 10, (B, C and D, respectively). The phenanthroline ligands decorate the planar arrays stretching outwards, either above or below the narrow 2D inorganic structures. By interdigitation of these protruding phen ligands of neighbouring planes, the 2D structures finally link into a 3D one (Fig. 3). The process, however, takes place in an unexpected way since the "gluing agent" is not, as usual in this type of arrangement, the $\pi\cdots\pi$ stacking interaction between adjacent phen groups but a number of non-conventional C—H$\cdots$O contacts instead, (Table 3) having phen C—H's as acceptors and (mainly) $O_{vanadyl}$ (entries 1–10 in Table 3) or $O_{phosphate}$ (entries 11–13 in Table 3) as donors.

3.1. The pseudo symmetry problem

The presence of eventual pseudo symmetry was something foreseeable "ab initio" from a careful observation of the diffraction data, which present an evident intensity systematics. Finding the law which describes these systematics, what would correspond to a reciprocal space approach to the problem, appeared however as non-trivial. The solution of the structure was attempted instead, looking for some noticeable pseudo symmetry aspects in the resulting model. This "direct space approach" proved to be successful, and the expected singularity prompted out as the threefold translational pseudo symmetry along the $\langle 1/3, -1/3, -1/6\rangle$ vector.

The pseudo operation was accurate for most of the structure including the phen molecules. The main deviation from a perfect match corresponded to the V2—O62, V5—O65 and V8—O68 groups, some of them disordered, which by the pseudo translation mixed up and loosed their otherwise well defined "identity" (V2 → V5; V5 → V8; V8 → V2).

In order to further investigate the degree of matching a transformation matrix leading to a "single motive cell" was used and this was found to be *M*: (1 0 0; 0 1 0; 1/3, −.1/3, −.1/6). This transformed the original cell into a rather deformed primitive one with $V' = 718.66\ (6)$ Å^3 = 1/6 V, and $a' = a = 10.6290\ (5)$ Å; $b' = b = 17.4275\ (8)$ Å; $c' = 8.0764\ (4)$ Å; $\alpha' = 135.229\ (3)°$; $\beta' = 57.374\ (4)°$; $\gamma' = \gamma = 91.995\ (4)°$. In this way, the *hkl* data set, consisting of the reflections which indices transformed into a set of integers, reduced to 1/3 of the original one. The other 2/3 of the total reflections, showed a much weaker intensity on average, but large enough as to confirm the original triple cell as the correct one, describing the structure under study.

The transformed model could be treated and refined in P-1 (**1b**), with inversion centres at the midpoint of all type B loops (Fig 2); loops A and A′ being equivalent through disorder. In this description, the pair V2/V2′ also appeared related by the inversion centre.

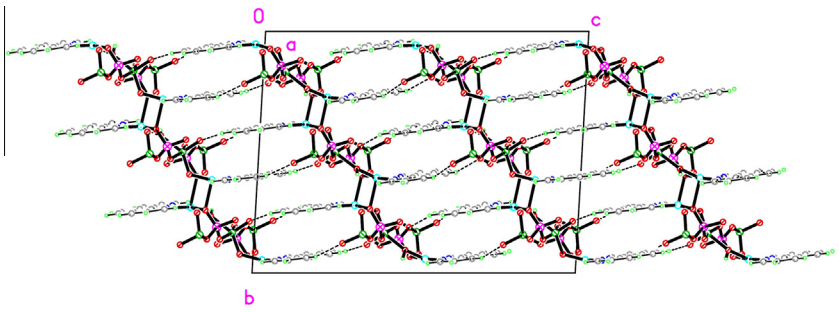

Fig. 3. View of the structure showing the interaction between interdigitated planar arrays, seen through their [1 0 0] projection as slanted 1D structures running from top-left to bottom-right. The inorganic framework drawn in heavy lines, phen groups in weak lines.

The net result was a reduction of the number of parameters by ca. 1/6, without jeopardizing the refinement performance (Table 1). Through all the procedure, the *R* indices and residual densities dropped appreciably. However, the model so refined suffered from a severe over simplification, showing only one type of disordered vanadyl group, now split into equally populated halves at both sides of an inversion centre.

Analysis of the results in Table 1 leads to the conclusion that the centrosymmetric sixfold cell is the proper one to correctly describe the "superstructure" in (**1a**), and this is confirmed in the differentiated disorder shown by the central V2, V5 and V8 atoms. However, if this effect is considered second order and accordingly disregarded, the system could be described by a much smaller cell, V′ = 1/6 V, with only half of a motive as the independent part and no substantial differences in its structural main features, but with loss of the finer details introduced by the "ordered" disorder scheme.

3.2. Comparison with related structures

Finn and Zubieta reported a structural study for a compound formulated as $[Cu(phen)(V^{V}O_2)(PO_4)]_2[V^{V}O_2(HO)]$ (**2**) [4], matching exactly the formulation of (**1b**). This compound was reported to crystallize in a triclinic cell, with half of a "single motive" (in the sense described so far in this paper) in the asymmetric unit. Unfortunately, no structural data seems to be available in the crystallographic data base (CSD) beyond the description in the paper, as to make any further comparison. On the other hand, a subsequent paper by Zhang et al. [5] describes what claimed to be an isostructural compound of (**2**) of slightly different formulation, $[Cu(phen)(V^{V}O_2)(PO_4)]_2[V^{IV}O_2(H_2O)]$ (**3**). Since structural data of this latter compound is available in the CSD, a comparison was in principle possible: the transformation *M* = (1 −1 1, 1 1 0, 0 1 0) drives the cell vectors of (**2**) and (**3**) into those in (**1b**), and the transformed model of (**3**) fits almost exactly onto (**1b**). Thus, it should be concluded that structures (**2**) and (**3**) coincide with the "average" description of (**1a**), and what we have called (**1b**).

Considering that both structures (**2**) and (**3**) appear as fairly accurate the possibility of a coincidental artefact in both, such as the overlooking of a large number of weak reflections must be considered as highly improbable, and consequently the models presented for (**2**) and (**3**) should be taken as basically correct.

The conclusion seems to be that $[Cu(phen)(V^{V}O_2)(PO_4)]_2[V^{V}O_2HO]$ can present some very subtle polymorphic states, of which (**1a**) and (**2**) are perhaps two out of a larger number, where the way in which a particular site is disordered allows it to "command" the long range order. This situation resembles the classic case of the Cu_3Au alloy which, when in its ordered phase, is simple cubic (P), with Au at (000) and Cu at (1/2,1/2,1/2), but face centred cubic (FCC) when completely disordered, with an "atom-per-site" of average composition 1/4(3Cu + Au) [15]. In the case of (**1a**) and (**2**), an evenly disordered state, which means a non-systematic distribution in space of the central VO_5polyhedra with opposite chirality, would lead to a small cell as in (**2**) and a unique 50%/50% split for the central V atom. Instead a partially ordered state, meaning some more systematic distribution in space of the central VO_5polyhedra with opposite chirality, can lead to much larger cells (sixfold in the case of (**1a**)). As stated before, intermediate situations cannot be disregarded from scratch.

3.3. Magnetic studies

The temperature dependence of χT observed for (**1a**) is displayed in Fig 4, already corrected for diamagnetism and TIP, which was estimated to be 3×10^{-3} emu mol^{-1}. The χT value at 300 K is 2.52 emu mol^{-1} K, which corresponds to six $S = ½$ centres with μ_B 1.83. This value is consistent with the spin only value of 1.73 μ_B

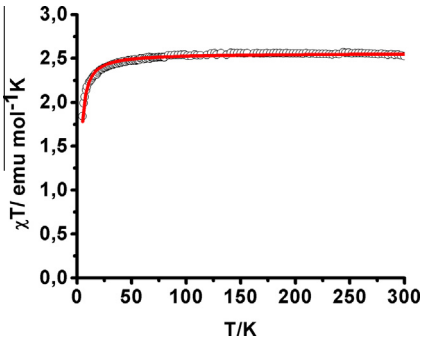

Fig. 4. Temperature dependence of χT for **1a**. Open circles represent the experimental magnetic susceptibility data; red line corresponds to the fit using the van Vleck analytical expression. (For interpretation of the references to colour in this figure legend, the reader is referred to the web version of this article.)

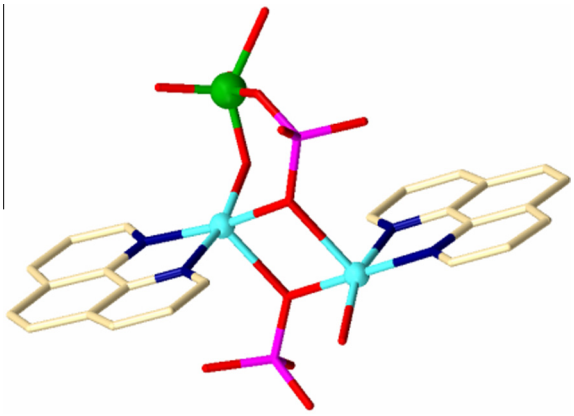

Scheme 2. Binuclear magnetic unit.

for an isolated Cu^{II} centre. At low temperatures the χT product decreases sharply; this phenomenon being explained as due to the presence of antiferromagnetic interactions. The low temperature limit for the χT value at 5 K is 1.84 emu mol^{-1} K. The inverse susceptibility in the high temperature range follows the Curie–Weiss law, with a Weiss constant θ of −0.7 K. The negative value of the Weiss constant makes evident the bulk antiferromagnetic interactions present at low temperatures in the studied 2D system.

Compound (**1a**) presents the shortest Cu···Cu distance of 3.262 (3) Å between Cu2 and Cu3 (Cu4 and Cu5). Taking into account that the other distances between the spin carriers are larger, the most relevant intramolecular super exchange interaction was defined between Cu2 and Cu3. This magnetic unit can be treated as a dinuclear system of Cu^{II} atoms bridged by μ_2,η^1-PO_4 groups (Scheme 2).

A fit of the corresponding magnetic data of (**1a**) was done, using the van Vleck equation for two $S = ½$ centres, $(H = -J\hat{S}_a \cdot \hat{S}_b)$ with the analytical expression given below:

$$\chi = \frac{2Ng^2\beta^2}{kT} \cdot \frac{e^{\frac{J}{kT}}}{1 + 3e^{\frac{J}{kT}}} \quad (1)$$

where *N* is Avogadro's number, β is the Bohr magneton and *k* the Boltzmann constant.

The parameters obtained by the fit of the experimental data using the above expression are $g = 2.1$ and $J = -3.51$ cm^{-1} ($R = 5 \times 10^{-4}$). The full line (red in the web, grey in print) in Fig 4 shows the fit of the experimental data, using these parameters. The obtained *J* value can be related to antiferromagnetic coupling, and suggests a weak transmission of the magnetic phenomenon

through the μ_2,η^1-PO_4 bridges. The bonds between both Cu^{II} centres occur through an equatorial–apical coordination mode. Since both copper centres present $d_{x^2-y^2}$ magnetic orbitals, the coordination mode does not allow a more effective overlap, and therefore a more intense antiferromagnetic exchange phenomenon.

The low value of J obtained for (**1a**) can be compared with that of $[Cu_2(bipy)_2(\mu_2,\eta^2\text{-}HPO_4)\text{–}(\mu_2,\eta^1\text{-}H_2PO_4)\ (\mu_2,\eta^2\text{-}H_2PO_4)]_n$ [16], where the two metal centres also have a square pyramidal geometry and are bridged by phosphate groups, with a Cu···Cu distance of 3.22 Å, forming a dinuclear system. Although, both experimental magnetic data were fitted using different analytical models, the obtained values of J are similar. For $[Cu_2(bipy)_2(\mu_2,\eta^2\text{-}HPO_4)\text{–}(\mu_2,\eta^1\text{-}H_2PO_4)\ (\mu_2,\eta^2\text{-}H_2PO_4)]_n$, $J = -5.3\ cm^{-1}$, a value which also indicates a weak antiferromagnetic behaviour produced by the same connectivity mode (equatorial–apical positions) between the metallic centres as in (**1a**). Only a few magnetic studies of phosphate-bridged Cu^{II} complexes are available in the literature. The work of Ainscough et al. shows that a μ_2,η^1-PO_4 bridge in an equatorial–axial coordination fashion between copper centres producing weak antiferromagnetism [17].

3.4. Conclusions

In the present work the studied compound $[Cu_6(phen)_6(V^VO_2)_6(PO_4)_6(V^VO_2HO)_3]$ (**1a**) was obtained by the hydrothermal method. The main conclusion is that $[Cu(phen)(V^VO_2)(PO_4)]_2[V^VO_2HO]$ motif can present some subtle polymorphic states, of which (**1a**) is perhaps one out of a larger number of related structures. In the present case the presence of a small vanadate disorder gives rise to a threefold translational pseudo symmetry, as the basis of this subtle superstructure difference. Even though there is a short Cu–Cu distance (3.262(3) Å), the apical-equatorial coordination mode of the bridging μ_2,η^1-PO_4 groups leads to a poor overlap of the magnetic orbitals and therefore to a weak antiferromagnetic phenomenon.

Acknowledgements

The authors acknowledge funding through projects FONDECYT 1080316 and Financiamiento Basal FB0807. The international collaboration Projects ECOS C08E02 and LIA-MIF CNRS 836 are also acknowledged. Authors are in debt with Thierry Guizouarn for the recording of the magnetic data. Authors also thank the financial support of ANPCyT (Project No. PME 2006-01113) for the purchase of the Oxford Gemini CCD diffractometer and the Spanish Research Council (CSIC) for provision of a free-of-charge licence to the Cambridge Structural Database.

Appendix A. Supplementary material

CCDC 924170 contains a Crystallographic Information File (CIF) for this structure. This file can be obtained free of charge from The Cambridge Crystallographic Data Centre via www.ccdc.cam.ac.uk/data_request/cif. Supplementary data associated with this article can be found, in the online version, at http://dx.doi.org/10.1016/j.molstruc.2013.08.005.

References

[1] S. Boudin, A. Guesdon, A. Leclaire, M.M. Borel, Int. J. Inorg. Mater. 2 (2000) 561–579.
[2] E. Le Fur, J.Y. Pivan, S. Ushak, D. Venegas-Yazigi, E. Spodine, Inorg. Chim. Acta 361 (2008) 1891–1896.
[3] S. Ushak, E. Spodine, D. Venegas-Yazigi, E. Le Fur, J.Y. Pivan, O. Peña, R. Cardoso-Gil, R. Kniep, J. Mater. Chem. 15 (2005) 4529–4534.
[4] R.C. Finn, J. Zubieta, J. Phys. Chem. Solids 62 (2001) 1513–1523.
[5] X.-M. Zhang, H.-S. Wu, S. Gao, X.-M. Chen, J. Solid State Chem. 176 (2003) 69–75.
[6] Y. Cui, Y. Xing, G. Li, Y. Liu, H. Meng, L. Liu, W. Pang, J. Solid State Chem. 177 (2004) 3080–3085.
[7] B-K. Koo, W. Ouellette, E. Burkholder, V. Golub, Ch. O'Connor, J. Zubieta, Solid State Sci. 6 (2004) 461–468.
[8] C-M. Wang, Y-L. Chuang, S.T. Chuang, K-H. Liia, J. Solid State Chem. 177 (2004) 2305–2310.
[9] D. Venegas-Yazigi, A. Vega, K. Valdés de la Barra, M. Saldías, E. Le Fur, Acta Cryst. C C68 (2012) m200–m202.
[10] S. Ushak, E. Spodine, D. Venegas-Yazigi, E. Le Fur, J.Y. Pivan, Micropor. Mesopor. Mater. 94 (2006) 50–55.
[11] Oxford Diffraction, in: CrysAlis PRO, Oxford Diffraction Ltd., Abingdon, Oxfordshire, England, 2009.
[12] G.M. Sheldrick, Acta Cryst. A64 (2008) 112–122.
[13] A.L. Spek, J. Appl. Cryst. 36 (2003) 7–13.
[14] A. Earnshaw, Introduction to Magnetochemistry, Academic Press, England, 1968.
[15] F.C. Nix, W. Shockley, Rev. Mod. Phys. 10 (1938) 1–71.
[16] P. Phuenghai, S. Youngme, N. Chaichit, C. Pakawaltchai, G.A. van Albada, M. Quesada, J. Reedijk, Polyhedron 25 (2006) 2198–2206.
[17] E.W. Ainscough, A.M. Brodie, J.D. Randford, J.M.J. Waters, J. Chem. Soc., Dalton (1997) 1251–1256.